

Design of Prefilters for Discrete Multiwavelet Transforms

Xiang-Gen Xia, Jeffrey S. Geronimo, Douglas P. Hardin, and Bruce W. Suter, *Senior Member, IEEE*

Abstract—The pyramid algorithm for computing single wavelet transform coefficients is well known. The pyramid algorithm can be implemented by using tree-structured multirate filter banks. In this paper, we propose a general algorithm to compute multiwavelet transform coefficients by adding proper premultirate filter banks before the vector filter banks that generate multiwavelets. The proposed algorithm can be thought of as a discrete vector-valued wavelet transform for certain discrete-time vector-valued signals. The proposed algorithm can be also thought of as a discrete multiwavelet transform for discrete-time signals. We then present some numerical experiments to illustrate the performance of the algorithm, which indicates that the energy compaction for discrete multiwavelet transforms may be better than the one for conventional discrete wavelet transforms.

I. INTRODUCTION

WAVELET transforms with single-mother wavelet functions have been studied extensively in the last ten years and are now well understood. One of their main properties is the time-frequency localization property of wavelet functions. However, it is known that there is a limitation for the time-frequency localization of a single wavelet function. Recently, multiwavelets have been studied, for example, [1]–[17], where several mother wavelet functions were used to expand a function. For instance, Geronimo, Hardin and Massopust [1] (GHM) constructed two scaling functions $\phi_1(t)$ and $\phi_2(t)$, and in [2] and [11] two related mother wavelets $\psi_1(t)$ and $\psi_2(t)$ are constructed. The scaling functions and associated wavelets are constructed so that $\phi_1(t - k_1)$, $\phi_2(t - k_2)$, $k_1, k_2 \in \mathbf{Z}$, are orthogonal, and the integer translations and the dilations of factor 2 of ψ_1 and ψ_2 form an orthonormal basis for $L^2(\mathbf{R})$. The two scaling functions ϕ_1 and ϕ_2 are supported in $[0, 1]$ and $[0, 2]$, respectively. Moreover, they are symmetric and Lipschitz continuous, see Fig. 1. This is impossible for single orthogonal wavelets, i.e., a single orthogonal wavelet cannot simultaneously have support $[0, 2]$, and be continuous, and a

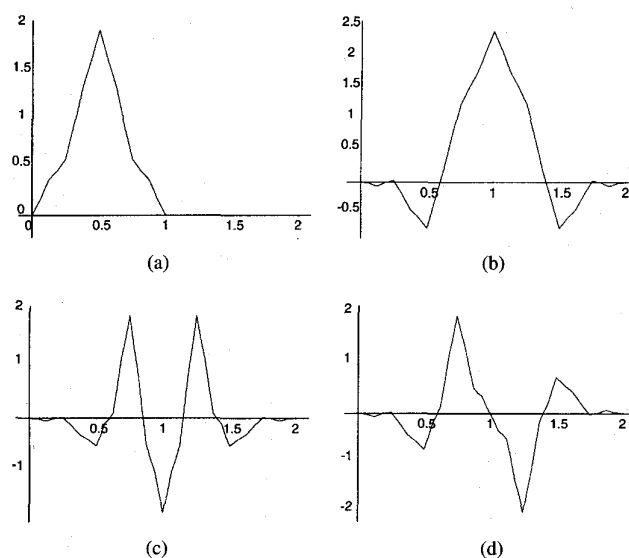


Fig. 1. Multiwavelets generated by Geronimo, Hardin, and Massopust: (a) and (b) are scaling functions $\phi_1(t)$ and $\phi_2(t)$, respectively; (c) and (d) are wavelet functions $\psi_1(t)$ and $\psi_2(t)$, respectively.

single orthogonal wavelet with compact support cannot have any symmetry.

For other orthogonal multiwavelets, see [2] and [3]. Another way to generate multiwavelets is using a vector/matrix-valued wavelet approach for vector/matrix-valued signals [8].

It is known that multiresolution analysis plays an important role in single-wavelet transforms. Similarly, multiresolution analysis is also very important in multiwavelet transforms, such as those associated with spline spaces [4]–[6], intertwining multiresolution analysis for multiwavelets [3], and vector-valued multiresolution analysis for vector-valued wavelets [8]. With multiresolution analysis structure wavelet transform coefficients with single mother wavelet function can be computed by using pyramid algorithms, such as Mallat's algorithm [20] and Shensa's algorithm [22]; also see, for example, [20]–[25]. These algorithms are based on the quadrature mirror filters $H(\omega)$ and $G(\omega)$ that generate scaling and mother wavelet functions. The algorithm structure can also be viewed as tree-structured multirate filter banks [18], [19], [30], [32], [33]. The rationale for these algorithms is that the samples $f(n/2^J)$ of a signal f for a large J are close to the orthogonal projection coefficients $c_{J,n}$ of f onto the multiresolution analysis space V_J . This, however, is no longer true for multiwavelets. In Section II, we will discuss it in more detail.

Manuscript received November 29, 1994; revised July 11, 1995. X.-G. Xia and B. W. Suter's work was supported in part by the Air Force Office of Scientific Research under Grant AFOSR-PO-94-0004, Grant AFOSR-PO-95-0004, and Grant AFOSR-616-95-0022. J. S. Geronimo's work was supported in part by a NSF grant. The associate editor coordinating the review of this paper and approving it for publication was Dr. Truong Q. Nguyen.

X.-G. Xia is with Information Sciences Laboratory, M/S RL96, Hughes Research Laboratories, Malibu, CA 90265 USA.

B. W. Suter is with the Department of Electrical and Computer Engineering, Air Force Institute of Technology, Wright-Patterson AFB, OH 45433-7765 USA.

J. S. Geronimo is with the Department of Mathematics, Georgia Institute of Technology, Atlanta, GA 30332 USA.

D. P. Hardin is with the Department of Mathematics, Vanderbilt University, Nashville, TN 37240 USA.

Publisher Item Identifier S 1053-587X(96)00686-X.

In this paper, we propose a pyramid algorithm for computing multiwavelet transform coefficients. The proposed algorithm is based on a pre and postconventional multirate filter bank and a tree-structured multirate vector filter bank [8], [9]. We investigate how the properties of the pre- and postfilters are reflected in the system as a whole. In particular we examine the relation between these filters and the lowpass and bandpass properties of the system. We call these filters, which provide a good match with the whole system, *good pre- and postfilters*. For any given multiwavelets, we are able to determine good prefilters associated to them, which are wavelet dependent.

Discrete vector-valued orthogonal wavelet transforms for vector-valued signals were introduced in [8], where the lowpass and bandpass properties for the vector quadrature mirror filters associated with vector-valued wavelets were interpreted similar to single wavelets, i.e., $\mathbf{H}(0)$ is identity and $\mathbf{G}(0)$ vanishes. In this case, prefiltering is not necessary but the conditions are restrictive. In this paper, we will also show that the proposed algorithm for computing multiwavelet transform coefficients can be thought of as a discrete vector-valued wavelet transform for certain vector-valued signals, where the highpass and bandpass properties are interpreted in a different way.

With the proposed algorithm, the multiwavelet series transform coefficients sometimes can not be computed exactly. In this paper, we present a necessary and sufficient condition for the exact computation. The proposed algorithm also suggests a discrete multiwavelet transform for discrete-time signals. In the last section, we present numerical experiments for the algorithm. The results show that better energy compaction can be achieved by using the proposed algorithm with good prefilters than the one by using the Daubechies wavelets D_4 . The energy compaction improvement is mainly due to the flexibility in choosing prefilters for multiwavelets so that some high-frequency components can be put into the low-frequency parts. Notice that an intuitive prefiltering procedure for the two wavelets generated by Geronimo, Hardin, and Massopust was also used by Heller *et al.* in [17] for image compression without much analysis. Discrete multiwavelet transforms without prefiltering appeared also in [13], [34], and [35], but no performance was discussed.

This paper is organized as follows. In Section II, we illustrate the motivation for the algorithm we want to propose, by making use of the scaling functions generated by Geronimo, Hardin and Massopust. In Section III, we introduce the algorithm and study its properties. In Section IV, we present some numerical experiments using the proposed algorithm.

II. MOTIVATION AND ANALYSIS FOR THE TWO-WAVELET CASE

Before going to the algorithm, we briefly review the scaling functions obtained by Geronimo, Hardin, and Massopust. The two scaling functions and their corresponding mother wavelet functions can be generated by the following matrix dilation equations [2] and [11]. Let

$$\begin{aligned} H_0 &= \begin{pmatrix} 3/10 & 2\sqrt{2}/5 \\ -\sqrt{2}/40 & -3/20 \end{pmatrix}, H_1 = \begin{pmatrix} 3/10 & 0 \\ 9\sqrt{2}/40 & 1/2 \end{pmatrix} \\ H_2 &= \begin{pmatrix} 0 & 0 \\ 9\sqrt{2}/40 & -3/20 \end{pmatrix}, H_3 = \begin{pmatrix} 0 & 0 \\ -\sqrt{2}/40 & 0 \end{pmatrix} \end{aligned} \quad (2.1)$$

and

$$\begin{aligned} G_0 &= \begin{pmatrix} -\sqrt{2}/40 & -3/20 \\ -1/20 & -3\sqrt{2}/20 \end{pmatrix}, G_1 = \begin{pmatrix} 9\sqrt{2}/40 & -1/2 \\ 9/20 & 0 \end{pmatrix} \\ G_2 &= \begin{pmatrix} 9\sqrt{2}/40 & -3/20 \\ -9/20 & 3\sqrt{2}/20 \end{pmatrix}, G_3 = \begin{pmatrix} -\sqrt{2}/40 & 0 \\ 1/20 & 0 \end{pmatrix}. \end{aligned} \quad (2.2)$$

Then, the two scaling function $\phi_1(t)$ and $\phi_2(t)$ in Fig. 1 can be generated via

$$\begin{pmatrix} \phi_1(t) \\ \phi_2(t) \end{pmatrix} = 2 \sum_{k=0}^3 H_k \begin{pmatrix} \phi_1(2t-k) \\ \phi_2(2t-k) \end{pmatrix}. \quad (2.3)$$

The two mother wavelet functions $\psi_1(t)$ and $\psi_2(t)$ can be constructed by

$$\begin{pmatrix} \psi_1(t) \\ \psi_2(t) \end{pmatrix} = 2 \sum_{k=0}^3 G_k \begin{pmatrix} \phi_1(2t-k) \\ \phi_2(2t-k) \end{pmatrix}. \quad (2.4)$$

Let V_j = closure of the linear span of $2^{j/2}\phi_l(2^j t - k)$, $l = 1, 2; k \in \mathbf{Z}$. With the above constructions, it has been proved that $\phi_l(t - k)$, $l = 1, 2; k \in \mathbf{Z}$ form an orthonormal basis for V_0 , and moreover the dilations and translations $2^{j/2}\psi_l(2^j t - k)$, $l = 1, 2; j, k \in \mathbf{Z}$ form an orthonormal basis for $L^2(\mathbf{R})$ [1], [2], [4]. In other words, the spaces V_j , $j \in \mathbf{Z}$, form an orthogonal multiresolution analysis of $L^2(\mathbf{R})$. Let

$$\mathbf{H}(\omega) = \sum_{k=0}^3 H_k e^{i\omega k}, \quad \mathbf{G}(\omega) = \sum_{k=0}^3 G_k e^{i\omega k}. \quad (2.5)$$

From the orthogonality, we have

$$\mathbf{H}(\omega)\mathbf{H}^\dagger(\omega) + \mathbf{H}(\omega + \pi)\mathbf{H}^\dagger(\omega + \pi) = I_2 \quad (2.6)$$

$$\mathbf{G}(\omega)\mathbf{G}^\dagger(\omega) + \mathbf{G}(\omega + \pi)\mathbf{G}^\dagger(\omega + \pi) = I_2 \quad (2.7)$$

$$\mathbf{H}(\omega)\mathbf{G}^\dagger(\omega) + \mathbf{H}(\omega + \pi)\mathbf{G}^\dagger(\omega + \pi) = 0_2 \quad (2.8)$$

where \dagger means the complex conjugate transpose, I_2 and 0_2 denote the 2×2 identity and all zero matrix, respectively.

Let $f \in V_0$, then,

$$\begin{aligned} f(t) &= \sum_{k \in \mathbf{Z}} (c_{1,0,k}\phi_1(t-k) + c_{2,0,k}\phi_2(t-k)) \quad (2.9) \\ &= \sum_{k \in \mathbf{Z}} (c_{1,J_0,k}2^{J_0/2}\phi_1(2^{J_0}t-k) \\ &\quad + c_{2,J_0,k}2^{J_0/2}\phi_2(2^{J_0}t-k)) \\ &\quad + \sum_{J_0 \leq j < \infty} \sum_{k \in \mathbf{Z}} (d_{1,j,k}2^{j/2}\psi_1(2^j t - k) \\ &\quad + d_{2,j,k}2^{j/2}\psi_2(2^j t - k)) \end{aligned} \quad (2.10)$$

where

$$c_{l,j,k} = \int f(t)2^{j/2}\phi_l(2^j t - k)dt \quad (2.11)$$

$$d_{l,j,k} = \int f(t)2^{j/2}\psi_l(2^j t - k)dt \quad (2.12)$$

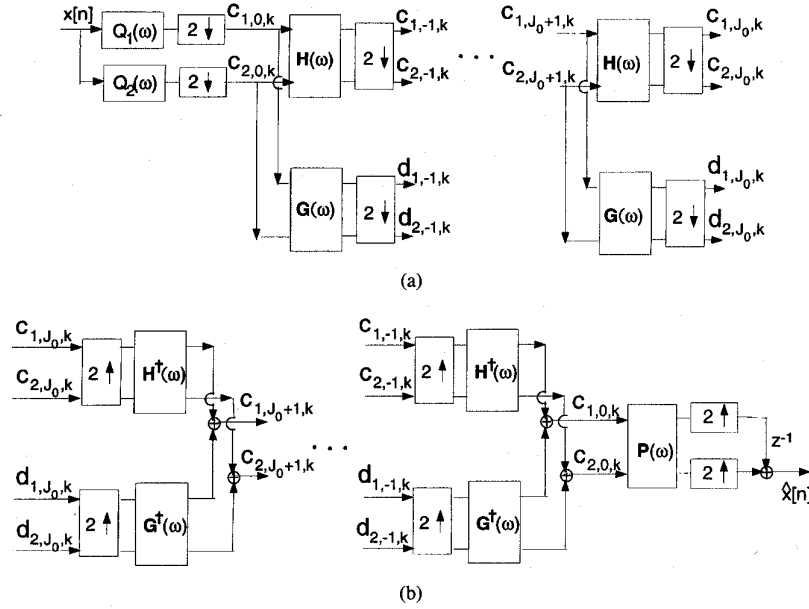


Fig. 2. Multiwavelet (a) decomposition; (b) reconstruction.

for $l = 1, 2; j, k \in \mathbf{Z}$ and $J_0 < 0$. By the dilation (2.3), (2.4), we have the following recursive relationship between the coefficients $(c_{1,j,k}, c_{2,j,k})^T$ and $(d_{1,j,k}, d_{2,j,k})^T$ where T means the transpose

$$\begin{pmatrix} c_{1,j-1,k} \\ c_{2,j-1,k} \end{pmatrix} = \sqrt{2} \sum_{n=0}^3 H_n \begin{pmatrix} c_{1,j,2k+n} \\ c_{2,j,2k+n} \end{pmatrix}, \quad j, k \in \mathbf{Z} \quad (2.13)$$

and

$$\begin{pmatrix} d_{1,j-1,k} \\ d_{2,j-1,k} \end{pmatrix} = \sqrt{2} \sum_{n=0}^3 G_n \begin{pmatrix} c_{1,j,2k+n} \\ c_{2,j,2k+n} \end{pmatrix}, \quad j, k \in \mathbf{Z}. \quad (2.14)$$

Moreover,

$$\begin{pmatrix} c_{1,j,n} \\ c_{2,j,n} \end{pmatrix} = \sqrt{2} \sum_{k=0}^3 \begin{pmatrix} H_k^\dagger \begin{pmatrix} c_{1,j-1,2k+n} \\ c_{2,j-1,2k+n} \end{pmatrix} \\ G_k^\dagger \begin{pmatrix} d_{1,j-1,2k+n} \\ d_{2,j-1,2k+n} \end{pmatrix} \end{pmatrix}. \quad (2.15)$$

The recursive (2.13) and (2.14) tell us that, to have all coefficients $c_{l,J_0,k}, d_{l,j,k}$ for $l = 1, 2; J_0 \leq j < 0, k \in \mathbf{Z}$ we only need to have coefficients $c_{l,0,k}$ for $l = 1, 2; k \in \mathbf{Z}$ in (2.9). This is exactly like the single-wavelet transforms [20]–[22], where we have single sequences $d_{j,k}$ and $c_{j,k}$ instead of pairs $(c_{1,j,k}, c_{2,j,k})$ and $(d_{1,j,k}, d_{2,j,k})$. It is known that in the single-wavelet transform case, the scaling function $\phi(t)$ has lowpass properties and $c_{J,k} \approx 2^{J/2} f(k/2^J)$ when J is large and f has certain smoothness (see, for example, [20], [23], [25]). Therefore, the single-wavelet transform coefficients $d_{j,k}, j < J, k \in \mathbf{Z}$ can be obtained from the samples $f(k/2^J), k \in \mathbf{Z}$ of f by using the pyramid algorithm. This is called Mallat algorithm [20]–[25]. For the detailed error analysis and improved algorithms, such as Shensa algorithm, of the above

approach for single-wavelet transform coefficient computation, see [23]–[25]. A natural question for multiwavelet transform coefficient computation is whether we can have the pair $(c_{1,J,k}, c_{2,J,k})$ for $k \in \mathbf{Z}$ from the samples of f . To analyze it, we go back to the representation (2.9) for $f(t)$. Since $\phi_1(t)$ is supported in $[0, 1]$ and $\phi_2(t)$ is supported in $[0, 2]$, $c_{l,0,k}$ for $l = 1, 2$ and $k \in \mathbf{Z}$ can be solved from $f(n/2)$ as follows [2]:

$$c_{2,0,k} = f(k+1)/\phi_2(1), \quad (2.16)$$

$$\begin{aligned} c_{1,0,k} &= f\left(\frac{2k+1}{2}\right) / \phi_1\left(\frac{1}{2}\right) \\ &\quad - f(k+1)\phi_2\left(\frac{1}{2}\right) / \left(\phi_2(1)\phi_1\left(\frac{1}{2}\right)\right) \\ &\quad - f(k)\phi_2\left(\frac{3}{2}\right) / \left(\phi_2(1)\phi_1\left(\frac{1}{2}\right)\right). \end{aligned} \quad (2.17)$$

Thus, with the recursive formulas (2.13), (2.14) one can exactly compute the wavelet coefficients $c_{l,J_0,k}, d_{l,j,k}$ for $l = 1, 2; J_0 \leq j < 0; k \in \mathbf{Z}$ from $f(n/2), n \in \mathbf{Z}$ when $f \in V_0$. This can be generalized to the J th resolution case: $c_{l,J_0,k}, d_{l,j,k}$ for $l = 1, 2, J_0 \leq j < J, k \in \mathbf{Z}$ from $f(n/2^J), n \in \mathbf{Z}$ when $f \in V_0$. For a signal f in $L^2(\mathbf{R})$ and sufficiently large J , f is approximately in V_J and the above computation may still be used.

With the formulas (2.15)–(2.17), one can reconstruct $f(n/2), n \in \mathbf{Z}$ from $c_{l,J_0,k}, d_{l,j,k}; l = 1, 2; J_0 \leq j < 0; k \in \mathbf{Z}$ as follows. With the coefficients $c_{l,J_0,k}, d_{l,j,k}$ we first reconstruct $f(n/2)$ from $c_{l,0,k}$

$$f(n) = c_{2,0,n-1}\phi_2(1) \quad (2.18)$$

$$\begin{aligned} f\left(\frac{2n+1}{2}\right) &= c_{1,0,n}\phi_1\left(\frac{1}{2}\right) + c_{2,0,n}\phi_2\left(\frac{1}{2}\right) \\ &\quad + c_{2,0,n-1}\phi_2\left(\frac{3}{2}\right). \end{aligned} \quad (2.19)$$

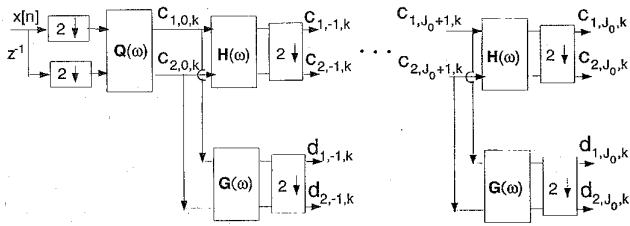
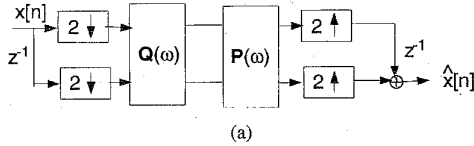
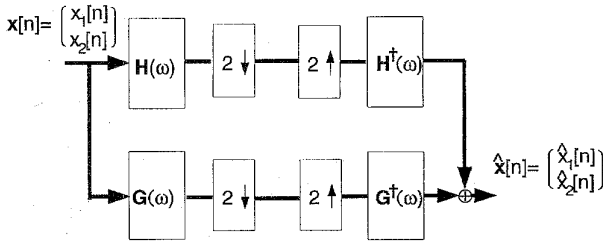


Fig. 3. Multiwavelet decomposition.



(a)



(b)

Fig. 4. (a) Conventional two-channel filter bank; (b) two-channel vector filter bank.

The coefficients $c_{l,0,k}$ can be reconstructed via (2.13)–(2.15).

Let

$$x[n] = f\left(\frac{n}{2}\right), n \in \mathbf{Z}$$

$$Q_1(\omega) = -\frac{\phi_2(\frac{3}{2})}{\phi_1(\frac{1}{2})\phi_2(1)} + \frac{1}{\phi_1(\frac{1}{2})}e^{i\omega} - \frac{\phi_2(\frac{1}{2})}{\phi_1(\frac{1}{2})\phi_2(1)}e^{i2\omega} \quad (2.20)$$

$$Q_2(\omega) = \frac{1}{\phi_2(1)}e^{i2\omega} \quad (2.21)$$

$$P(\omega) = \begin{pmatrix} 0 & 0 \\ \phi_1(\frac{1}{2}) & \phi_2(\frac{1}{2}) \end{pmatrix} + \begin{pmatrix} 0 & \phi_2(1) \\ 0 & \phi_2(\frac{3}{2}) \end{pmatrix}e^{-i\omega}. \quad (2.22)$$

Then, the above decomposition and reconstruction can be represented by a modified tree-structured vector filter bank shown in Figs. 2(a) and (b), respectively. Notice that the above procedure was used in [17] in image compression applications.

Let $Q(\omega)$ be the polyphase matrix of $Q_1(\omega)$ and $Q_2(\omega)$ with sampling rate 2, i.e.,

$$Q(\omega) = \begin{pmatrix} -\frac{\phi_2(3/2)}{\phi_1(1/2)\phi_2(1)} - \frac{\phi_2(1/2)}{\phi_1(1/2)\phi_2(1)}e^{i\omega} & \frac{1}{\phi_1(1/2)} \\ \frac{1}{\phi_2(1)}e^{i2\omega} & 0 \end{pmatrix}. \quad (2.23)$$

Then, the decomposition part in Fig. 2(a) can be redrawn in Fig. 3. Thus, the decomposition and reconstruction in Figs. 2 and 3 can be split into two separate systems as shown in Fig. 4, where the one in (a) is a conventional two-channel filter bank and the one in (b) is a two-channel vector filter bank [9]. We have the following straightforward result.

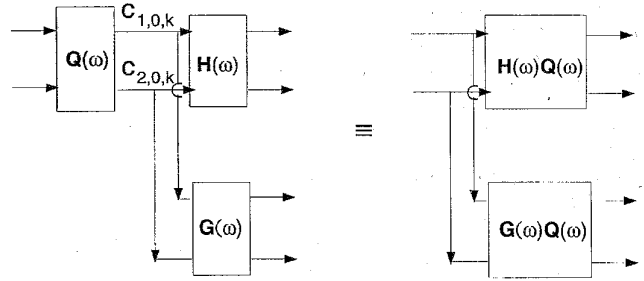


Fig. 5. Equivalent systems.

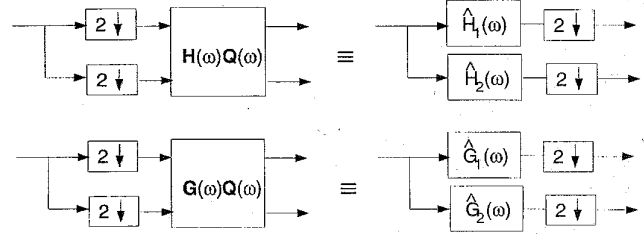
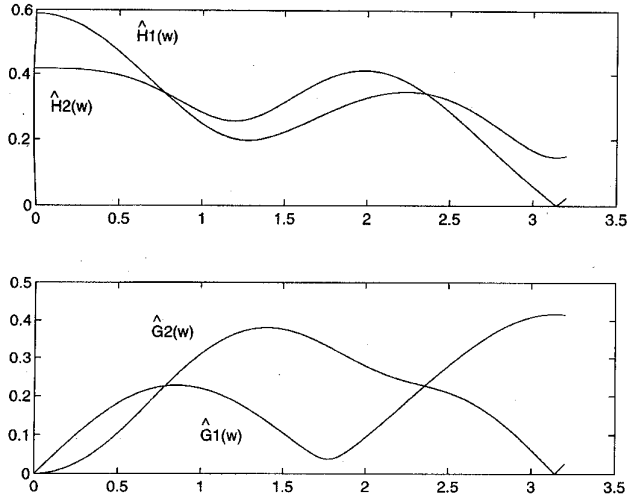


Fig. 6. Equivalence of polyphase and nonpolyphase representations.

Proposition 1: The perfect reconstruction property of the system in Fig. 2 is equivalent to the perfect reconstruction properties of the two systems in Fig. 4(a) and (b).

With the identities (2.6)–(2.8), the system in Fig. 4(b) is perfect reconstruction. It is also easy to check $Q(\omega)P(\omega) = I_2$ with $Q(\omega)$ defined in (2.23) and $P(\omega)$ defined in (2.22). Thus, we have $\hat{x}[n] = x[n]$, i.e., the system in Fig. 2 gives perfect reconstruction. When the matrix quadrature mirror filters $H(\omega)$ and $G(\omega)$ satisfying (2.6)–(2.8) are fixed, Proposition 1 also tells us that the system in Fig. 2 still gives perfect reconstruction as long as the system in Fig. 4(a) gives perfect reconstruction. This suggests that one may use other polyphase matrixes $Q(\omega)$ and $P(\omega)$ rather than the ones in (2.23) and (2.22). This allows much freedom for choosing $Q(\omega)$ and $P(\omega)$. Which one is desired? To study this question, we restudy the system in Fig. 3. The prefilter polyphase matrix $Q(\omega)$ can be absorbed into the one behind it as shown in Fig. 5, where $H(\omega)Q(\omega)$ is the polyphase matrix of another two filters $\hat{H}_1(\omega)$ and $\hat{H}_2(\omega)$, and $\hat{G}_1(\omega)$, $\hat{G}_2(\omega)$ are similar (see Fig. 6). The frequency responses of these four filters are shown in Fig. 7. Since we usually need to decompose the outputs of the filtering of $\hat{H}_l(\omega)$, $l = 1, 2$, we may want that $\hat{H}_l(\omega)$, $l = 1, 2$, have lowpass properties. Since the outputs of the filtering of $\hat{G}_l(\omega)$, $l = 1, 2$, are kept for quantization, we usually expect $\hat{G}_l(\omega)$, $l = 1, 2$, to have bandpass property so that only a small amount of the outputs are significant. From Fig. 7, one can see that $\hat{H}_1(\omega)$ is not a good lowpass filter because it doesn't vanish at π . Constructing good lowpass filters $\hat{H}_l(\omega)$ and good bandpass filters $\hat{G}_l(\omega)$ for $l = 1, 2$ is one of the main goals of the next section.

The solvability (2.16), (2.17) of $c_{l,0,k}$ from $f(n/2)$ in (2.9) is very special due to the fact that there are only two scaling functions supported in $[0, 1]$ and $[0, 2]$, respectively. This solvability may fail for general N wavelets. In the next section, we present a necessary and sufficient condition for

Fig. 7. $|\hat{H}_l(\omega)|$ and $|\hat{G}_l(\omega)|$ for $l = 1, 2$.

the solvability in N wavelet case. When $c_{l,0,k}$ cannot be solved from the samples $f(n/M)$, we lack a system like the one in Fig. 2 to exactly compute the multiwavelet series transform coefficients from the samples. In this case, there are no associated pre- or postfilters $\mathbf{Q}(\omega)$ and $\mathbf{P}(\omega)$ like the above two-wavelet case. We then have to use other pre- or postfilters $\mathbf{Q}(\omega)$ and $\mathbf{P}(\omega)$ such that $\mathbf{Q}(\omega)\mathbf{P}(\omega) = I_N$. We also use the low bandpass criterion to choose these pre- or postfilters.

III. A GENERAL ALGORITHM

In this section, we first generalize the analysis in Section II from the two-wavelet case to N wavelet case. We then study the conditions and properties on prefilters.

A. Solvability of the Transform Coefficients from Samples

We consider general orthogonal N wavelets with compact support, where there are N compactly supported scaling functions $\phi_l(t)$, $l = 1, 2, \dots, N$, and N mother wavelet functions $\psi_l(t)$, $l = 1, 2, \dots, N$, where $\phi_l(t - k)$, $k \in \mathbf{Z}$, $l = 1, 2, \dots, N$ are mutually orthogonal, and $2^{j/2}\psi_l(2^j t - k)$, $j, k \in \mathbf{Z}$, $l = 1, 2, \dots, N$ form an orthonormal basis for $L^2(\mathbf{R})$. Let $\mathbf{H}(\omega)$ and $\mathbf{G}(\omega)$ be their corresponding $N \times N$ matrix quadrature mirror filters with impulse responses H_k and G_k , $k \in \mathbf{Z}$, respectively. Let

$$\Phi(t) \triangleq (\phi_1(t) \dots \phi_N(t))^T, \quad \Psi(t) \triangleq (\psi_1(t) \dots \psi_N(t))^T.$$

Then, we have the following matrix dilation equations

$$\Phi(t) = 2 \sum_k H_k \Phi(2t - k) \quad (3.1)$$

$$\Psi(t) = 2 \sum_k G_k \Phi(2t - k). \quad (3.2)$$

For each fixed $j \in \mathbf{Z}$, let V_j be the closure of the linear span of $2^{j/2}\phi_l(2^j t - k)$, $l = 1, 2, \dots, N$; $k \in \mathbf{Z}$. Then, the spaces V_j , $j \in \mathbf{Z}$ form an orthogonal multiresolution analysis for $L^2(\mathbf{R})$. Although we only focus on two-band multiwavelets, the theory developed in this section can be easily generalized

to M -band wavelets where there are N scaling functions and $(M - 1)N$ mother wavelet functions.

Let $f \in V_0$, then,

$$\begin{aligned} f(t) &= \sum_{l=1}^N \sum_{k \in \mathbf{Z}} c_{l,0,k} \phi_l(t - k) \quad (3.3) \\ &= \sum_{l=1}^N \sum_{k \in \mathbf{Z}} c_{l,J_0,k} 2^{J_0/2} \phi_l(2^{J_0} t - k) \\ &\quad + \sum_{l=1}^N \sum_{J_0 \leq j < 0} \sum_{k \in \mathbf{Z}} d_{l,j,k} 2^{j/2} \psi_l(2^j t - k) \quad (3.4) \end{aligned}$$

where $J_0 < 0$ and $c_{l,j,k}$, $d_{l,j,k}$ are defined by (2.11), (2.12). Let $\mathbf{c}_{j,k} \triangleq (c_{1,j,k} \dots c_{N,j,k})^T$ and $\mathbf{d}_{j,k} \triangleq (d_{1,j,k} \dots d_{N,j,k})^T$. Then, similar to (2.13)–(2.15), we have the following decomposition and reconstruction

$$\mathbf{c}_{j-1,k} = \sqrt{2} \sum_n H_n \mathbf{c}_{j,2k+n} \quad (3.5)$$

$$\mathbf{d}_{j-1,k} = \sqrt{2} \sum_n G_n \mathbf{c}_{j,2k+n} \quad (3.6)$$

and

$$\mathbf{c}_{j,n} = \sqrt{2} \sum_k (H_k \mathbf{c}_{j-1,2k+n} + G_k \mathbf{d}_{j-1,2k+n}). \quad (3.7)$$

Thus, to determine the wavelet coefficients $\mathbf{c}_{J_0,k}$ and $\mathbf{d}_{j,k}$ for $J_0 \leq j < 0, k \in \mathbf{Z}$ from the samples of $f(t)$, it is only necessary to determine the coefficients $\mathbf{c}_{0,k}$ for $k \in \mathbf{Z}$ from the samples of $f(t)$.

Suppose we have samples $f(n/M)$ of $f(t)$ with sampling rate $1/M$. Let $x[n] \triangleq f(n/M)$, $n \in \mathbf{Z}$,

$$X(\omega) = \sum_n x[n] e^{-i\omega n}, \quad X_m(\omega) = \sum_n x[Mn + m] e^{-i\omega n} \quad (3.8)$$

where $X_m(\omega)$ is the m th polyphase component of $X(\omega)$ for $m = 0, 1, \dots, M - 1$. Let

$$\begin{aligned} P_{m,l}(\omega) &= \sum_n \phi_l \left(\frac{m}{M} + n \right) e^{-in\omega}, \\ l &= 1, 2, \dots, N, \quad m = 0, 1, \dots, M - 1, \quad (3.9) \end{aligned}$$

and

$$C_{l,j}(\omega) = \sum_k c_{l,j,k} e^{-ik\omega}, \quad l = 1, 2, \dots, N, j \in \mathbf{Z}. \quad (3.10)$$

Let $\mathbf{P}(\omega)$ be the following $M \times N$ matrix function

$$\mathbf{P}(\omega) = \begin{pmatrix} P_{0,1}(\omega) & P_{0,2}(\omega) & \dots & P_{0,N}(\omega) \\ P_{1,1}(\omega) & P_{1,2}(\omega) & \dots & P_{1,N}(\omega) \\ \dots & \dots & \dots & \dots \\ P_{M-1,1}(\omega) & P_{M-1,2}(\omega) & \dots & P_{M-1,N}(\omega) \end{pmatrix}. \quad (3.11)$$

The Fourier transform of (3.3) with $t = \frac{m}{M} + n$, $m = 0, 1, \dots, M - 1$ yields

$$(X_0(\omega), \dots, X_{M-1}(\omega))^T = \mathbf{P}(\omega) (C_{1,0}(\omega) \dots C_{N,0}(\omega))^T. \quad (3.12)$$

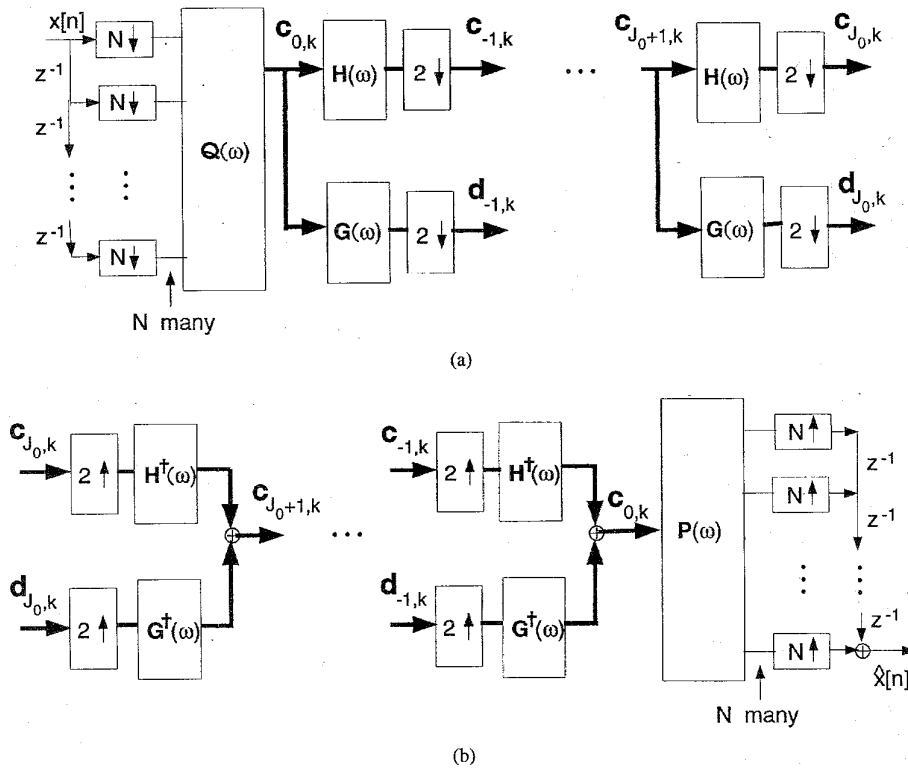


Fig. 8. Discrete multiwavelet transform: (a) Decomposition; (b) reconstruction.

Since all $\phi_l(t)$, $l = 1, 2, \dots, N$ are assumed of compact support, all entries of the matrix function $\mathbf{P}(\omega)$ are polynomials of $e^{-i\omega}$. By (3.12), we have the following result on the solvability.

Proposition 2: The wavelet transform coefficients $c_{j_0,k}$ and $d_{j_0,k}$ for $J_0 \leq j < 0, k \in \mathbf{Z}$ can be exactly computed from $f(n/M)$, $n \in \mathbf{Z}$, if and only if $M \geq N$ and the rank of the matrix $\mathbf{P}(\omega)$ in (3.11) is always N for all $\omega \in [0, 2\pi)$.

Since we usually need to use efficient sampling, the sampling rate should be as small as possible. Thus, based on Proposition 2, we assume $M = N$ in what follows. In this case, we have

Corollary 1: The wavelet transform coefficients $c_{j_0,k}$ and $d_{j_0,k}$ for $J_0 \leq j < 0, k \in \mathbf{Z}$ can be exactly computed from $f(n/N)$, $n \in \mathbf{Z}$, if and only if the determinant function of the matrix function $\mathbf{P}(\omega)$ does not have any zeroes for $\omega \in [0, 2\pi)$, i.e., the inverse of $\mathbf{P}(\omega)$ exists. The inverse of $\mathbf{P}(\omega)$ is FIR, i.e., finite impulse response, if and only if the determinant of $\mathbf{P}(\omega)$ is $ce^{im_0\omega}$ for a certain nonzero constant c and a certain integer m_0 .

Clearly, the matrix function $\mathbf{P}(\omega)$ in (2.22) satisfies Corollary 1. Actually, the matrix $\mathbf{Q}(\omega)$ in (2.23) is its inverse.

Let $\mathbf{Q}(\omega)$ be the inverse of $\mathbf{P}(\omega)$, i.e., $\mathbf{P}(\omega)\mathbf{Q}(\omega) = I_N$. Then the decomposition and reconstruction of $c_{j,k}$ and $d_{j,k}$ from $f(n/N)$ can be shown by the diagram in Fig. 8. With the system in Fig. 8, we have the following result on the perfect reconstruction similar to the one in Section II.

Proposition 3: The system in Fig. 8 is perfect reconstruction, i.e., $\hat{x}[n] = x[n]$, if and only if the matrix quadrature mirror filters $\mathbf{H}(\omega)$ and $\mathbf{G}(\omega)$ satisfy (2.6)–(2.8) with I_2 and

0_2 replaced by I_N and 0_N respectively, and $\mathbf{P}(\omega)\mathbf{Q}(\omega) = I_N$.

When we only consider a discrete-time signal $x[n]$, Proposition 3 also suggests that one may use other pre- or postfilters $\mathbf{Q}(\omega)$ and $\mathbf{P}(\omega)$ rather than the one in (3.12). Thus, for fixed $\mathbf{H}(\omega)$ and $\mathbf{G}(\omega)$, there are many algorithms in terms of different $\mathbf{Q}(\omega)$ and $\mathbf{P}(\omega)$. Which one is good? Similar to the argument at the end of Section II, we prefer that the combined filter $\mathbf{H}(\omega)\mathbf{Q}(\omega)$ has the lowpass property and $\mathbf{G}(\omega)\mathbf{Q}(\omega)$ has the bandpass property. Recall that an $N \times N$ matrix filter $\mathbf{F}(\omega)$ is also a polyphase matrix of N filters $F_1(\omega), \dots, F_N(\omega)$ (see, for example, [32]). One way to interpret the lowpass and bandpass property of a matrix filter $\mathbf{F}(\omega)$ is to use the lowpass and bandpass property of its associated N filters $F_l(\omega)$, $l = 1, 2, \dots, N$.

Let $\mathbf{H}(\omega)\mathbf{Q}(\omega)$ be the polyphase matrix of $\hat{H}_l(\omega)$, $l = 1, 2, \dots, N$ and $\mathbf{G}(\omega)\mathbf{Q}(\omega)$ be the polyphase matrix of $\hat{G}_l(\omega)$, $l = 1, 2, \dots, N$. In the following, we study the conditions on $\mathbf{Q}(\omega)$ and $\mathbf{P}(\omega)$ given $\mathbf{H}(\omega)$ and $\mathbf{G}(\omega)$ such that

$$\hat{H}_l(\pi) = 0, \quad l = 1, 2, \dots, N \quad (3.13)$$

$$\hat{G}_l(0) = 0, \quad l = 1, 2, \dots, N. \quad (3.14)$$

In the case that (3.13) and (3.14) can not be satisfied, we consider the following relaxed conditions on $\mathbf{Q}(\omega)$ and $\mathbf{P}(\omega)$ given $\mathbf{H}(\omega)$ and $\mathbf{G}(\omega)$

$$\hat{H}_l(\pi) = \epsilon_l, \quad l = 1, 2, \dots, N \quad (3.15)$$

$$\hat{G}_l(0) = \delta_l, \quad l = 1, 2, \dots, N \quad (3.16)$$

where ϵ_l and δ_l , $l = 1, 2, \dots, N$ are predesigned small numbers if they are not 0. The conditions (3.15) and (3.16) can

be interpreted as a tiny loss at high frequency π of $\hat{H}_l(\omega)$ and a tiny loss at low frequency 0 of $\hat{G}_l(\omega)$. The prefilters $\mathbf{Q}(\omega)$ that have inverses $\mathbf{P}(\omega)$, determinants $\det(\mathbf{Q}(0)) = \pm 1$, and satisfy (3.13), (3.14) or (3.15), (3.16), are called *good prefilters* with respect to $\mathbf{H}(\omega)$ and $\mathbf{G}(\omega)$. For the prefilter $\mathbf{Q}(\omega)$ in (2.23) in Section II, one can easily check that $\delta_1 = \delta_2 = 0$, $\epsilon_1 = 0.1473$, $\epsilon_2 = 0$, and $\det(\mathbf{Q}(0)) = -0.1535$.

B. Existence and Construction of Good Prefilters

First, we formulate $\hat{H}_l(\omega)$ and $\hat{G}_l(\omega)$. Let

$$\mathbf{H}(\omega) = (H_{mn}(\omega))_{N \times N}, \quad \mathbf{G}(\omega) = (G_{mn}(\omega))_{N \times N},$$

$$\mathbf{Q}(\omega) = (Q_{mn}(\omega))_{N \times N}.$$

Then (see [32] and [33])

$$\hat{H}_l(\omega) = \sum_{m=1}^N \left(\sum_{k=1}^N H_{lk}(N\omega) Q_{km}(N\omega) \right) e^{-i(m-1)\omega}, \quad (3.17)$$

$$\hat{G}_l(\omega) = \sum_{m=1}^N \left(\sum_{k=1}^N G_{lk}(N\omega) Q_{km}(N\omega) \right) e^{-i(m-1)\omega}. \quad (3.18)$$

Thus

$$\hat{H}_l(\pi) = \sum_{m=1}^N \left(\sum_{k=1}^N H_{lk}(N\pi) Q_{km}(N\pi) \right) (-1)^{m-1} \quad (3.19)$$

$$\hat{G}_l(0) = \sum_{m=1}^N \left(\sum_{k=1}^N G_{lk}(0) Q_{km}(0) \right). \quad (3.20)$$

Rearrange the summation in (3.19) and (3.20)

$$\hat{H}_l(\pi) = \sum_{k=1}^N H_{lk}(N\pi) \sum_{m=1}^N Q_{km}(N\pi) (-1)^{m-1} \quad (3.21)$$

$$\hat{G}_l(0) = \sum_{k=1}^N G_{lk}(0) \sum_{m=1}^N Q_{km}(0). \quad (3.22)$$

When N is even, (3.21) becomes

$$\hat{H}_l(\pi) = \sum_{k=1}^N H_{lk}(0) \sum_{m=1}^N Q_{km}(0) (-1)^{m-1}. \quad (3.23)$$

Therefore, to have a good prefilter $\mathbf{Q}(\omega)$ with respect to $\mathbf{H}(\omega)$ and $\mathbf{G}(\omega)$ we only need to solve for $\mathbf{Q}(0)$ from (3.13) and (3.14) or (3.15) and (3.16); and from (3.22) and (3.23), with $\det(\mathbf{Q}(0)) = \pm 1$. Then we form $\mathbf{Q}(\omega) = \mathbf{Q}(0)\mathbf{V}(\omega)$ or $\mathbf{Q}(\omega) = \mathbf{V}(\omega)\mathbf{Q}(0)$, where $\mathbf{V}(\omega) = \mathbf{I}_N$, or

$$\mathbf{V}(\omega) = (\mathbf{I}_N + (e^{i\omega} - 1)\mathbf{v}_\rho \mathbf{v}_\rho^\dagger) \cdots (\mathbf{I}_N + (e^{i\omega} - 1)\mathbf{v}_1 \mathbf{v}_1^\dagger) \quad (3.24)$$

for high order prefilters, where \mathbf{v}_j is an $N \times 1$ constant vector with $\mathbf{v}_j^\dagger \mathbf{v}_j = 1$; $j = 1, 2, \dots, \rho$. With $\mathbf{Q}(\omega)$ as above its inverse is given by $\mathbf{P}(\omega) = \mathbf{V}^\dagger(\omega)\mathbf{Q}^{-1}(0)$ or $\mathbf{P}(\omega) = \mathbf{Q}^{-1}(0)\mathbf{V}^\dagger(\omega)$ (see [32] and [33]).

When N is odd, (3.21) is

$$\hat{H}_l(\pi) = \sum_{k=1}^N H_{lk}(\pi) \sum_{m=1}^N Q_{km}(\pi) (-1)^{m-1}. \quad (3.25)$$

In this case, we first need to solve for $\mathbf{Q}(0)$ from (3.13) and (3.23) or (3.15) and (3.23), with $\det(\mathbf{Q}(0)) = \pm 1$. Then we

use the form of $\mathbf{Q}(\omega) = \mathbf{Q}(0)\mathbf{V}(\omega)$ or $\mathbf{Q}(\omega) = \mathbf{V}(\omega)\mathbf{Q}(0)$ with $\mathbf{V}(\omega)$ in (3.24), and substitute $\mathbf{Q}(\pi)$ in (3.25). Finally we solve for \mathbf{v}_j , $j = 1, 2, \dots, \rho$ from (3.14) or (3.16) and (3.25).

We next have a complete analysis of the $N = 2$ case.

Proposition 4: Suppose $N = 2$, i.e., two-wavelet case. If a good prefilter $\mathbf{Q}(\omega)$ exists that satisfies (3.13) and (3.14) and has an inverse $\mathbf{P}(\omega)$, then both $\mathbf{H}(0)$ and $\mathbf{G}(0)$ are singular. Conversely, if $\mathbf{H}(0)$ and $\mathbf{G}(0)$ are both singular and $c_1\mathbf{H}(0) \neq c_2\mathbf{G}(0)$ for any constants c_1 and c_2 , then a good prefilter $\mathbf{Q}(\omega)$ exists that satisfies (3.13) and (3.14) and has an inverse $\mathbf{P}(\omega)$. If $\mathbf{H}(0)$ and $\mathbf{G}(0)$ are both singular and $c_1\mathbf{H}(0) = c_2\mathbf{G}(0)$ for some constants c_1 and c_2 , then there do not exist any good prefilters.

Proof: Equations (3.22) and (3.23) are

$$\hat{G}_l(0) = G_{l1}(0)(Q_{11}(0) + Q_{12}(0))$$

$$+ G_{l2}(0)(Q_{21}(0) + Q_{22}(0)), \quad l = 1, 2$$

$$\hat{H}_l(\pi) = H_{l1}(0)(Q_{11}(0) - Q_{12}(0))$$

$$+ H_{l2}(0)(Q_{21}(0) - Q_{22}(0)), \quad l = 1, 2.$$

If $\mathbf{H}(0)$ or $\mathbf{G}(0)$ is nonsingular, then, by (3.13), (3.14), $Q_{11}(0) = Q_{12}(0)$, $l = 1, 2$, or $Q_{11}(0) = -Q_{12}(0)$, $l = 1, 2$. This implies that $\mathbf{Q}(0)$ is singular, i.e., no inverse of $\mathbf{Q}(\omega)$ exists. This proves the first part of the proposition.

If $\mathbf{H}(0)$ and $\mathbf{G}(0)$ are both singular, then, by (3.13) and (3.14) and without loss of generality

$$Q_{11}(0) - Q_{12}(0) = a_1(Q_{21}(0) - Q_{22}(0))$$

$$Q_{11}(0) + Q_{12}(0) = a_2(Q_{21}(0) + Q_{22}(0))$$

where $a_1 \neq 0$ and $a_2 \neq 0$ are two constants. If $c_1\mathbf{H}(0) \neq c_2\mathbf{G}(0)$ for any constants c_1 and c_2 , then, $a_1 \neq a_2$. Thus, $\mathbf{Q}(0)$ with determinant ± 1 exists. This proves the second part of the proposition.

When $\mathbf{H}(0)$ and $\mathbf{G}(0)$ are both singular and $c_1\mathbf{H}(0) = c_2\mathbf{G}(0)$ for two constants c_1 and c_2 , the conditions (3.13) and (3.14) imply $a_1 = a_2$ in the above equations and $Q_{1l}(0) = a_1 Q_{2l}(0)$ for $l = 1, 2$. Therefore, $\mathbf{Q}(0)$ is singular and $\mathbf{Q}(\omega)$ does not have an inverse. From the singularities of both matrixes $\mathbf{H}(0)$ and $\mathbf{G}(0)$, the conditions (3.15) and (3.16) cannot be satisfied for ϵ_l and δ_l , $l = 1, 2$ that are not all zero. This proves the last part of the proposition. \square

When $\mathbf{H}(0)$ and $\mathbf{G}(0)$ are both nonsingular, then we consider a prefilter satisfying (3.15) and (3.16). In this case,

$$Q_{l1}(0) - Q_{l2}(0) = c_{l1}\epsilon_1 + c_{l2}\epsilon_2, \quad l = 1, 2$$

$$Q_{l1}(0) + Q_{l2}(0) = d_{l1}\delta_1 + d_{l2}\delta_2, \quad l = 1, 2$$

where ϵ_l and δ_l , $l = 1, 2$ are small numbers and the c_{lk} and d_{lk} are the elements of $(\mathbf{H}(0))^{-1}$ and $(\mathbf{G}(0))^{-1}$. Therefore, $Q_{nm}(0)$ are also small. Thus, the condition $\det(\mathbf{Q}(0)) = \pm 1$ is impossible. This proves the following result.

Proposition 5: When $\mathbf{H}(0)$ and $\mathbf{G}(0)$ are both nonsingular, there do not exist any good prefilters, where $N = 2$.

We now investigate the case when one of $\mathbf{H}(0)$ and $\mathbf{G}(0)$ is singular and the other one is nonsingular.

When $\mathbf{H}(0)$ is nonsingular, let

$$\mathbf{H}^{-1}(0) = \begin{pmatrix} a & b \\ c & d \end{pmatrix}.$$

By (3.23) and (3.15)

$$\begin{pmatrix} Q_{11}(0) - Q_{12}(0) \\ Q_{21}(0) - Q_{22}(0) \end{pmatrix} = \mathbf{H}^{-1}(0) \begin{pmatrix} \epsilon_1 \\ \epsilon_2 \end{pmatrix} = \begin{pmatrix} a\epsilon_1 + b\epsilon_2 \\ c\epsilon_1 + d\epsilon_2 \end{pmatrix}. \quad (3.26)$$

Let $\delta_1 = \delta_2 = 0$. Since $\mathbf{G}(0)$ is singular, (3.16) is equivalent to

$$c_1(Q_{11}(0) + Q_{12}(0)) + d_1(Q_{21}(0) + Q_{22}(0)) = 0 \quad (3.27)$$

where c_1 and d_1 are two constants. By (3.26) and (3.27), there exists $Q_{nm}(0)$, $m, n = 1, 2$, such that (3.15) and (3.16) are satisfied and, moreover, $\det(\mathbf{Q}(0)) = \pm 1$.

When $\mathbf{G}(0)$ is nonsingular, we let $\epsilon_1 = \epsilon_2 = 0$ and Proposition 6 follows.

Proposition 6: Suppose $N = 2$. When one and only one of $\mathbf{H}(0)$ and $\mathbf{G}(0)$ is singular, there exists a good prefilter $\mathbf{Q}(\omega)$ such that $\det(\mathbf{Q}(0)) = \pm 1$, and $|\hat{H}_l(\pi)|$ and $|\hat{G}_l(0)|$, $l = 1, 2$, can be made arbitrarily small.

We now go back to the two-wavelet case in Section II. For the multiwavelets in Section II,

$$\mathbf{H}(0) = \begin{pmatrix} \frac{3}{5} & \frac{2\sqrt{2}}{5} \\ \frac{2\sqrt{2}}{5} & \frac{1}{5} \end{pmatrix} \quad \text{and} \quad \mathbf{G}(0) = \begin{pmatrix} \frac{2\sqrt{2}}{5} & -\frac{4}{5} \\ 0 & 0 \end{pmatrix}.$$

Since $\mathbf{H}(0)$ is nonsingular, there is no good prefilter $\mathbf{Q}(\omega)$ that satisfies (3.13) and (3.14) and has an inverse. However, we may consider the relaxed conditions (3.15) and (3.16) and use Proposition 6. In this case, the equations (3.26) and (3.27) become

$$\begin{aligned} Q_{11}(0) - Q_{12}(0) &= -\epsilon_1 + 2\sqrt{2}\epsilon_2, \\ Q_{21}(0) - Q_{22}(0) &= 2\sqrt{2}\epsilon_1 - 3\epsilon_2, \\ Q_{11}(0) + Q_{12}(0) &= \sqrt{2}(Q_{21}(0) + Q_{22}(0)). \end{aligned}$$

Let $Q_{11}(0) + Q_{12}(0) = x$, then

$$\mathbf{Q}(0) = \begin{pmatrix} \frac{x - \epsilon_1 + 2\sqrt{2}\epsilon_2}{2} & \frac{x + \epsilon_1 - 2\sqrt{2}\epsilon_2}{2} \\ \frac{x + 4\epsilon_1 - 3\sqrt{2}\epsilon_2}{2\sqrt{2}} & \frac{x - 4\epsilon_1 + 3\sqrt{2}\epsilon_2}{2\sqrt{2}} \end{pmatrix} \quad (3.28)$$

and $\det(\mathbf{Q}(0)) = x(5\sqrt{2}\epsilon_2 - 5\epsilon_1)/(2\sqrt{2})$. Thus, $\det(\mathbf{Q}(0)) = \pm 1$ implies

$$x = \pm \frac{2\sqrt{2}}{5(\sqrt{2}\epsilon_2 - \epsilon_1)}. \quad (3.29)$$

This tells us that, if we substitute the value of x in (3.29) into (3.28), $\mathbf{Q}(\omega)$ is a good prefilter with $\hat{H}_l(\pi) = \epsilon_l$ and $\hat{G}_l(0) = 0$ for $l = 1, 2$, where ϵ_1 and ϵ_2 are arbitrarily given. One can also impose the orthogonality for $\mathbf{Q}(0)$. In this case, the prefilter may be paraunitary and the whole multiwavelet transform is orthogonal.

Two numerical examples for $|\hat{H}_l(\omega)|$ and $|\hat{G}_l(\omega)|$ are shown in Fig. 9 with $\epsilon_1 = 0$ and $\epsilon_2 = 0.01$, and in Fig. 10 with $\epsilon_1 = 0$ and $\epsilon_2 = 0.1$, where $\mathbf{Q}(\omega) = \mathbf{Q}(0)$ for all ω . The choice of ϵ_1 and ϵ_2 here is just arbitrary. Although ϵ_l can be made arbitrarily small, the coefficients in $\hat{H}_l(\omega)$ and $\hat{G}_l(\omega)$ may be large. To choose good parameters, ϵ_l depends on practical problems. The optimal choice of ϵ_l needs further investigation. From Figs. 9 and 10, one can see that all magnitudes of the frequency responses of the filters $\hat{H}_l(\omega)$ and $\hat{G}_l(\omega)$ at high

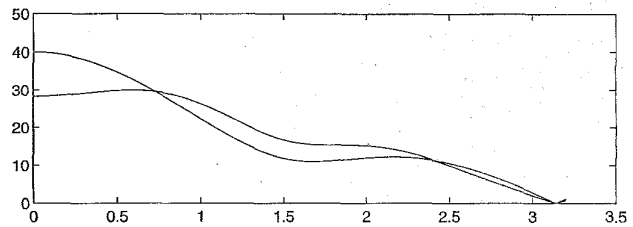


Fig. 9. (a) $|\hat{H}_l(\omega)|$, $l = 1, 2$; (b) $|\hat{G}_l(\omega)|$, $l = 1, 2$, where $\epsilon_1 = 0$ and $\epsilon_2 = 0.01$.

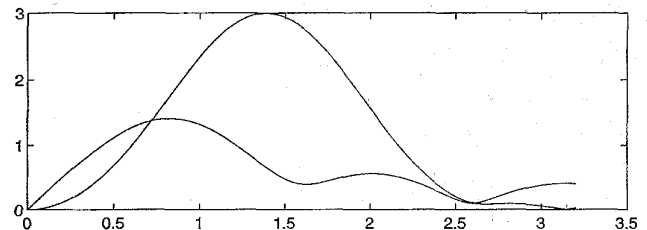
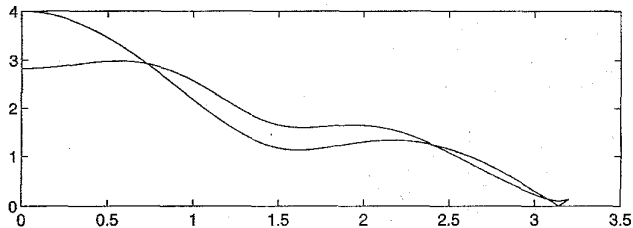


Fig. 10. (a) $|\hat{H}_l(\omega)|$, $l = 1, 2$; (b) $|\hat{G}_l(\omega)|$, $l = 1, 2$, where $\epsilon_1 = 0$ and $\epsilon_2 = 0.1$.

frequency are small. This implies that the high-frequency part in a decomposition of a signal will be suppressed, so that some of them are moved into the low-frequency parts while the perfect reconstruction of the signal from the decomposition is still possible. It is, however, impossible for single wavelets, where the lowpass and highpass filters $H(\omega)$ and $G(\omega)$ are complementary filters. This is exactly the reason why the energy compaction ratio can be significantly improved with multiwavelet transforms. We will see this property in the numerical examples in the next section.

C. Discrete Vector-Valued Wavelet Transform Point of View

Given two matrix filters $\mathbf{H}(\omega)$ and $\mathbf{G}(\omega)$ that satisfy (2.6)–(2.8) with I_2 and O_2 replaced by I_N and O_N , respectively, the discrete vector-valued wavelet transform associated with them is defined in [8] by the diagram shown in Fig. 11, where $\mathbf{x}[n] = (x_1[n], \dots, x_N[n])^T$.

Thus, the multiwavelet transform in Fig. 8 can be thought of as the discrete vector-valued wavelet transform for the vector-valued signal $\mathbf{x}[n]$ that is the output of the linear system $\mathbf{Q}(\omega)$ with the vector-valued input signal $(x[Nn], x[Nn - 1], \dots, x[Nn - N + 1])^T$.

IV. NUMERICAL EXAMPLES OF MULTIWAVELET TRANSFORMS

In this section, we want to implement the proposed algorithm in Sections II and III and compare the results with

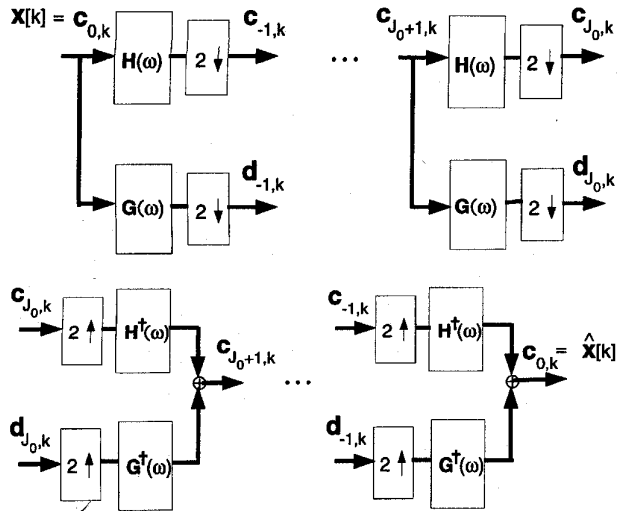


Fig. 11. (a) Discrete vector-valued wavelet transform; (b) inverse discrete vector-valued wavelet transform.

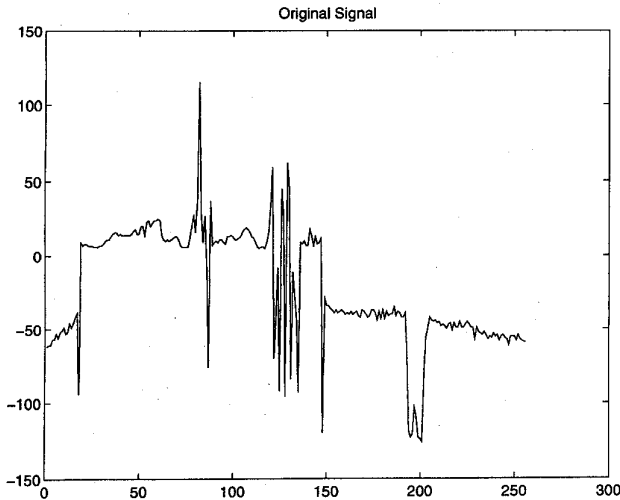


Fig. 12. Test signal.

those obtained from the conventional wavelet transform with Daubechies D_4 basis.

The test signal we use is the 100th horizontal line of the Cameraman.256 image, shown in Fig. 12. We decompose it with two-step wavelet transforms and multiwavelet transforms, i.e., $J_0 = -2$ in Fig. 8. Signals shown in Figs. 13–16 are decomposed signals of the test signal, where signals from 1 to 64 are the lowpass parts and signals from 65 to 265 are the bandpass parts. The multiwavelets we use are those obtained by Geronimo, Hardin, and Massopust and are discussed in Sections II and III.

Let MWT stand for multiwavelet transform and WT stand for wavelet transform. Fig. 13 shows the decomposition by using MWT without prefiltering, i.e., $\mathbf{Q}(\omega) = I_N$ in Fig. 8. Fig. 14 shows the decomposition by using the MWT with the prefilter $\mathbf{Q}(\omega)$ in (2.23). Fig. 15 shows the decomposition by using MWT with the prefilter $\mathbf{Q}(\omega) = \mathbf{Q}(0)$ in (3.28) with $\epsilon_1 = 0$ and $\epsilon_2 = 0.1$. Fig. 16 shows the decomposition by using conventional WT with Daubechies D_4 coefficients. One

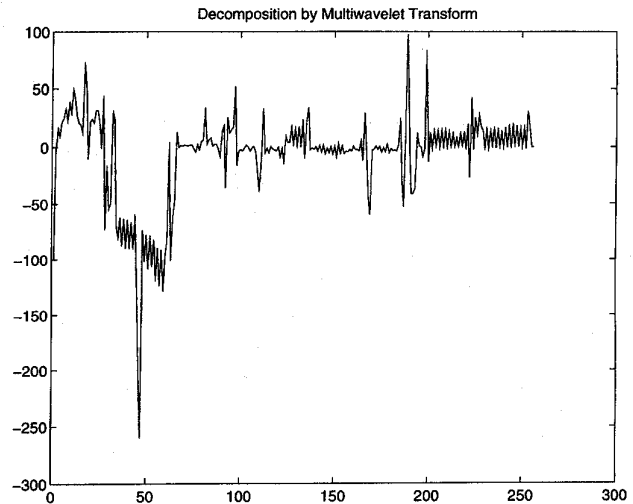


Fig. 13. Decomposition using MWT without prefiltering.

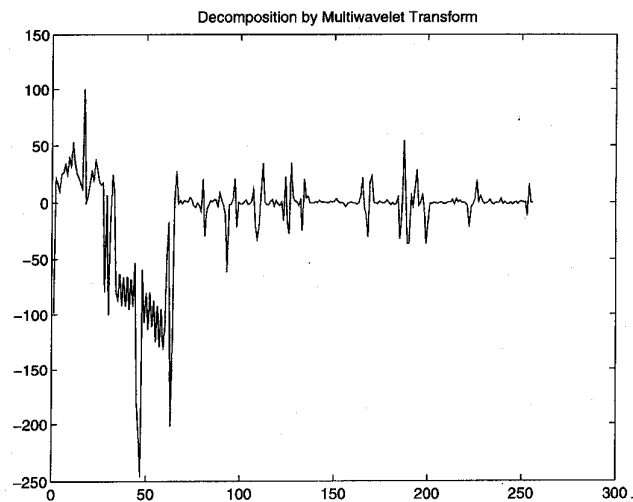


Fig. 14. Decomposition using MWT with prefiltering $\mathbf{Q}(\omega)$ in (2.23).

can see from Figs. 13–15 the improvement of the prefiltering process in the implementation of MWT. One can also see that some high-frequency signals are included in the lowpass parts of MWT in Figs. 13–15, and the bandpass parts in Figs. 14 and 15 are smoother than the one in Fig. 16 with Daubechies D_4 basis. This tells us that more information is concentrated in the lowpass part of MWT, while the perfect reconstruction from the decomposition signals is still maintained. This can also be seen from the energy compaction ratios shown in Table I. The energy compaction ratio r in this case (two-step decomposition) is defined by the ratio of the energy of the bandpass parts over the total energy of the signal

$$r \triangleq \frac{\sum_{n=65}^{256} |y[n]|^2}{\sum_{n=1}^{256} |y[n]|^2}$$

where $y[n]$ is the MWT of the test signal. The reason behind it is due to the small magnitudes of the filters $\hat{H}_l(\omega)$ and $\hat{G}_l(\omega)$ at high frequencies, see Fig. 10. From our numerical

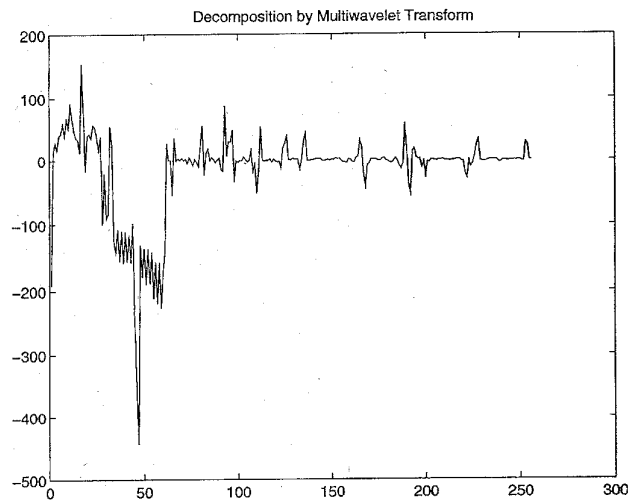


Fig. 15. Decomposition using MWT with prefiltering $\mathbf{Q}(\omega)$ in (3.28) with $\epsilon_1 = 0$ and $\epsilon_2 = 0.1$.

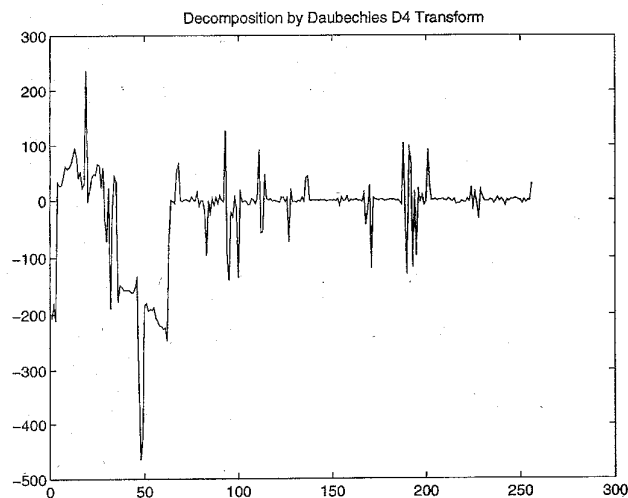


Fig. 16. Decomposition using WT with Daubechies D_4 basis.

TABLE I
ENERGY COMPACTION RATIO

	r
MWT with $\mathbf{Q}(\omega) = I_N$	0.1374
MWT with $\mathbf{Q}(\omega)$ in (2.23) with $\epsilon_1 = 0.1473$ and $\epsilon_2 = 0$	0.0575
MWT with $\mathbf{Q}(\omega)$ in (3.28) with $\epsilon_1 = 0$ and $\epsilon_2 = 0.1$	0.0453
WT with Daubechies D_4	0.1123

experiments, the energy compaction ratio is not sensitive to the small changes of the parameters ϵ_i .

V. CONCLUSION

In this paper, we introduced a pyramid algorithm for the implementation of multiwavelet transforms by adding a pre- and postfilter to a tree-structured vector filter bank. The algorithm also suggests a discrete multiwavelet transform for discrete-time signals. We obtained a necessary and sufficient condition for the exact determination of the multiwavelet transform

coefficients from the samples of signals. We also studied some properties of a prefilter, such as lowpass and bandpass properties. We analyzed and constructed good prefilters. Our numerical examples showed that the decomposition by using the proposed algorithm with good prefiltering has better energy compaction than the one with Daubechies D_4 wavelets. The main reason is that the frequency responses of all the filters $\hat{\mathbf{H}}_l(\omega)$ and $\hat{\mathbf{G}}_l(\omega)$ for multiwavelet transforms are significantly smaller at high frequencies compared to the peaks at other frequencies and, moreover, the perfect reconstruction is still maintained. This is, however, impossible for the filters for single wavelets (orthogonal or biorthogonal wavelets). This suggests its potential applications in image/video compression.

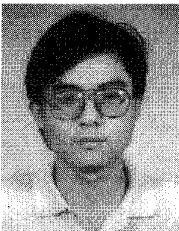
ACKNOWLEDGMENT

The authors would like to thank the anonymous reviewers for their detailed comments and one reviewer who pointed out an error in the proof of Proposition 4 in the original version of this manuscript. They would also like to thank C. Heil and M. Smith for various discussions on filter bank theory.

REFERENCES

- [1] J. S. Geronimo, D. P. Hardin, and P. R. Massopust, "Fractal functions and wavelet expansions based on several scaling functions," *J. Approx. Theory*, 1994.
- [2] G. Donovan, J. S. Geronimo, D. P. Hardin, and P. R. Massopust, "Construction of orthogonal wavelets using fractal interpolation functions," preprint, 1994.
- [3] G. Donovan, J. S. Geronimo, and D. P. Hardin, "Intertwining multiresolution analysis and the construction of piecewise polynomial wavelets," preprint, 1994.
- [4] T. N. T. Goodman, S. L. Lee, and W. S. Tang, "Wavelets in wandering subspaces," *Trans. Amer. Math. Soc.*, vol. 338, pp. 639–654, 1993.
- [5] T. N. T. Goodman and S. L. Lee, "Wavelets of multiplicity r ," *Trans. Amer. Math. Soc.*, vol. 342, pp. 307–324, Mar. 1994.
- [6] L. Hervé, "Multi-resolution analysis of multiplicity d : Applications to dyadic interpolation," *Appl. Comput. Harmonic Anal.*, vol. 1, pp. 299–315, 1994.
- [7] C. A. Micchelli and Y. Xu, "Using the matrix refinement equation for the construction of wavelets on invariant sets," *Appl. Comput. Harmonic Anal.*, vol. 1, pp. 391–401, 1994.
- [8] X.-G. Xia and B. W. Suter, "Vector-valued wavelets and vector filter banks," preprint, 1994.
- [9] ———, "Multirate filter banks with block sampling," preprint, 1994.
- [10] G. Strang and V. Strela, "Orthogonal multiwavelets with vanishing moments," *J. Opt. Eng.*, vol. 33, pp. 2104–2107, 1994.
- [11] ———, "Short wavelets and matrix dilation equations," *IEEE Trans. Signal Processing*, vol. 43, no. 1, pp. 108–115, Jan. 1995.
- [12] G. G. Walter, "Orthogonal finite element multiwavelets," preprint, 1994.
- [13] M. Vetterli and G. Strang, "Time-varying filter banks and multiwavelets," in *Proc. Sixth Digital Signal Processing Workshop*, Yosemite, CA, USA, Oct. 1994.
- [14] R. Q. Jia and Z. Shen, "Multiresolution analysis and wavelets," preprint 1994.
- [15] C. Heil, G. Strang, and V. Strela, "Approximation by translates of refinable functions," preprint, 1994.
- [16] C. Heil and D. Colella, "Matrix refinement equations: Existence and uniqueness," preprint, 1994.
- [17] P. N. Heller *et al.*, "Multiwavelet filter banks for data compression," preprint, 1994.
- [18] M. Vetterli and C. Herley, "Wavelets and filter banks: Theory and design," *IEEE Trans. Signal Processing*, vol. 40, pp. 2207–2232, Sept. 1992.
- [19] O. Rioul and M. Vetterli, "Wavelets and signal processing," *IEEE Signal Processing Mag.*, pp. 14–38, Oct. 1991.
- [20] S. Mallat, "Multifrequency channel decompositions of images and wavelet methods," *IEEE Trans. Acoust. Speech, Signal Processing*, vol. 37, pp. 2091–2110, 1989.

- [21] O. Rioul and P. Duhamel, "Fast algorithms for discrete and continuous wavelet transforms," *IEEE Trans. Inform. Theory*, vol. 38, pp. 569–586, Mar. 1992.
- [22] M. J. Shensa, "The discrete wavelet transform: Wedding the Atrous and Mallat algorithm," *IEEE Trans. Signal Processing*, vol. 40, pp. 2464–2482, Oct. 1992.
- [23] X.-G. Xia, "Topics in wavelet transforms," Ph.D. dissertation, Dept. of Elect. Eng.–Syst., Univ. Southern Calif., Los Angeles, USA, 1992.
- [24] X.-G. Xia and Z. Zhang, "On sampling theorem, wavelets and wavelet transforms," *IEEE Trans. Signal Processing*, vol. 41, pp. 3524–3535, Dec. 1993.
- [25] X.-G. Xia, C.-C. J. Kuo, and Z. Zhang, "Wavelet coefficient computation with optimal prefiltering," *IEEE Trans. Signal Processing*, vol. 42, pp. 2191–2197, Aug. 1994.
- [26] R. Balian, "Un principe d'incertitude fort en théorie du signal ou en mécanique quantique," *C. R. Acad. Sc.*, Paris, vol. 292, série 2, pp. 1357–1362, 1987.
- [27] F. Low, "Complete sets of wave-packets," in *A Passion for Physics: Essays in Honor of Geoffrey Chew*. Singapore: World Scientific, 1985, pp. 17–22.
- [28] I. Daubechies, "The wavelet transform, time-frequency localization and signal analysis," *IEEE Trans. Inform. Theory*, vol. 36, pp. 961–1005, Sept. 1990.
- [29] ———, "Orthonormal bases of compactly supported wavelets," *Comm. Pure Appl. Math.*, vol. 41, pp. 909–996, 1988.
- [30] ———, Ten lectures on wavelets, *Ten Lectures on Wavelets*. Philadelphia: SIAM, 1992.
- [31] C. K. Chui, *An Introduction to Wavelets*. New York: Academic, 1992.
- [32] P. P. Vaidyanathan, *Multirate Systems and Filter Banks*. Englewood Cliffs, NJ: Prentice-Hall, 1993.
- [33] M. Vetterli and J. Kovačević, *Wavelets and Subband Coding*. Englewood Cliffs, NJ: Prentice-Hall, 1995.
- [34] P. Rieder, J. Götze and J. A. Nossek, "Algebraic design of discrete multiwavelet transforms," in *Proc. IEEE ICASSP*, Adelaide, Australia, Apr. 1994.
- [35] ———, "Multiwavelet transforms based on several scaling functions," in *Proc. IEEE Int. Symp. Time-Frequency Time-Scale Anal.*, Philadelphia, PA, Oct. 1994.



Xiang-Gen Xia received the B.S. degree in mathematics from Nanjing Normal University, Nanjing, China, the M.S. degree in mathematics from Nankai University, Tianjin, China, and the Ph.D. degree in electrical engineering from the University of Southern California, Los Angeles, USA, in 1983, 1986, and 1992, respectively.

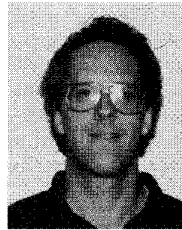
He was an assistant professor at Nankai University during 1986–1988, a teaching assistant at the University of Cincinnati, Cincinnati, OH, USA, during 1988–1990, a research assistant at the University of Southern California, Los Angeles, USA, during 1990–1992, and a research scientist at the Air Force Institute of Technology during 1993–1994. He is currently a research staff member at Hughes Research Laboratories, Malibu, CA, USA. His current research interests include wavelet transforms and multirate filterbanks: theory and applications in signal/image processing, wireless communications, and channel/source coding; time-frequency analysis and synthesis; and numerical analysis and inverse problems in signal/image processing.



He is a member of SIAM, the AMS, and the MAA.

Jeffrey S. Geronimo was born in Cairo, Egypt in 1949. He received the B.S. degree from The State University of New York, Albany, USA, in 1972, and a Ph.D. in physics from Rockefeller University, New York City, USA, in 1977.

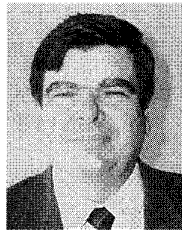
He has been with the School of Mathematics at Georgia Institute of Technology, Atlanta, GA, USA, since 1977, except for a two-year visit to the Centre de Physique Theorique at Saclay, France. His areas of interest include orthogonal polynomials, fractals, and wavelets.



Douglas P. Hardin was born in 1958. He received the B.E.E. from Georgia Institute of Technology, Atlanta, USA, in 1980, the M.S. in electrical engineering from Stanford University, Stanford, CA, USA, in 1982, and the Ph.D. in mathematics from Georgia Institute of Technology in 1985.

He has been with the department of mathematics at Vanderbilt University, Nashville, TN, USA, since 1986. His areas of interest include image processing, fractals, and wavelets.

He is a member of SIAM and the AMS.



Bruce W. Suter (S'80–M'85–SM'92) received the B.S. and M.S. degrees in electrical engineering in 1972, and the Ph.D. degree in computer science in 1988, all from the University of South Florida, Tampa, USA.

Since 1989, he has been with the Graduate School of Engineering at the Air Force Institute of Technology, Wright-Patterson AFB, OH, USA, where he is an associate professor in the Department of Electrical and Computer Engineering. He also serves as associate editor of *IEEE TRANSACTIONS ON SIGNAL PROCESSING*. His current research interests include wavelet analysis, multirate signal processing, and time-frequency analysis. His professional background includes design experience with Honeywell Inc., St. Petersburg, FL, USA, and with Litton Industries, Woodland Hills, CA, USA. He has academic experience at the University of Alabama at Birmingham, USA.

Dr. Suter is a member of Tau Beta Pi and Eta Kappa Nu.